Acid-labile mPEG-Vinyl Ether-1,2-Dioleylglycerol Lipids with Tunable pH Sensitivity: Synthesis and Structural Effects on Hydrolysis Rates, DOPE Liposome Release Performance and Pharmacokinetics

Junhwa Shin[a,^], **Pochi Shum**[a,+], **Jessica Grey**[a,-], **Shin-ichi Fujiwara**[a,#], **Guarov S. Malhotra**[b], **Andres González-Bonet**[a], **Seok-Hee Hyun**[a], **Elaine Moase**[b], **Theresa M. Allen**[b], and **David H. Thompson**[a,*]

[a]Department of Chemistry, Purdue University, 560 Oval Drive, West Lafayette, Indiana 47907-1393, USA

[b]University of Alberta, Department of Pharmacology, 9-31 Medical Sciences Building, Edmonton, AB T6G 2H7, CANADA

Abstract

A family of 3-methoxypoly(ethylene glycol)-vinyl ether-1,2-dioleylglycerol (mPEG-VE-DOG) lipopolymer conjugates, designed on the basis of DFT calculations to possess a wide range of proton affinities, was synthesized and tested for their hydrolysis kinetics in neutral and acidic buffers. Extruded ~100 nm liposomes containing these constructs in 90 mol% 1,2-dioleoyl-*sn*-glycero-3-phosphoethanolamine (DOPE) produced dispersions that retained their calcein cargo for more than 2 days at pH 7.5, but released the encapsulated contents over a wide range of timescales as a function of the electronic properties of the vinyl ether linkage, the solution pH and the mPEG-VE-DOG composition in the membrane. The *in vivo* performance of two different 90:10 DOPE:mPEG-VE-DOG compositions was also evaluated for blood circulation time and biodistribution in mice, using ^{125}I-tyraminylinulin as a label. The pharmacokinetic profiles gave a $T_{1/2}$ of 7 h and 3 h for 90:10 DOPE:ST302 and 90:10 DOPE:ST502, respectively, with the liposomes being cleared predominantly by liver and spleen uptake. The behavior of these DOPE:mPEG-VE-DOG formulations is consistent with their relative rates of vinyl ether hydrolysis, i.e., the more acid-sensitive mPEG-VE-DOG derivatives produce faster leakage rates from DOPE:mPEG-VE-DOG liposomes, but decreased the blood circulation times in mice. These findings suggest that the vinyl ether-based PEG-lipid derivatives are promising agents for stabilizing acid-sensitive DOPE liposomes to produce formulations with *a priori* control over their pH-responsiveness in vitro. Our data also suggest, however, that the same factors that contribute to enhanced acid-sensitivity of the DOPE:mPEG-VE-DOG dispersions are also likely responsible for their reduced pharmacokinetic profiles.

Keywords

mPEG-Lipid; Vinyl ether hydrolysis; Drug delivery; dePEGylation

INTRODUCTION

Since Bangham's original discovery of lipid myelin figures,[1] liposomes have progressively evolved to a clinically-proven, commercially successful nanoscale carrier system for delivering high concentrations of small molecule agents.[2] They are attractive delivery vehicles because they can be [1] fabricated from naturally occurring lipids with excellent biocompatibility properties; [2] created with chemical gradients across the membrane bilayer that enable the encapsulation of high drug concentrations within unilamellar liposomes via "remote loading"[3-6] to encapsulate a wide variety of drugs or imaging agents, e.g., doxorubicin,[3] topotecan,[7] mitomycin C,[8] As_2O_3,[9, 10] and ^{64}Cu;[11] [3] rapidly and simply produced on large scale with controlled diameters;[12] [4] formulated with different discrete, well-characterized components to provide enhanced permeation and retention,[13-15] active targeting,[16-21] intracellular trafficking and endosomal escape,[10, 19, 22-24] and imaging capabilities;[25] and [5] utilized for the delivery of water-soluble and water-insoluble active pharmaceutical agents in the liposome core and shell, respectively, without requiring chemical modification.

In many cases, liposome formulations suffer from non-optimal rates of drug release at the target site.[26-28] Numerous efforts have been directed toward resolving the release rate limitations, leading to the advent of PEG-grafted liposome formulations that incorporate bioactivation strategies that exploit exchange processes[29-35] or the unique environments present within acidic tumors and/or intracellular compartments (e.g., endosomal activation via thiol-,[36-38] enzyme-,[39] or acid-sensitive[40-47] triggering schemes). These systems are designed to be stable in the circulation at pH 7.4, but lose their structural integrity and impermeability upon activation at the target site. Rapid contents release by these triggering events can impart a greater therapeutic effect than conventional liposomal drug formulations, since the active agent is released more rapidly and at higher concentrations within the target cell environment.[21] Unfortunately, most of these approaches are formulation-specific and lack the general compositional flexibility that would be afforded by a structure-guided molecular design approach.

Cleavable PEG-moieties, grafted onto fusogenic DOPE liposomes, offer a means to achieve this goal via liposome dePEGylation[23, 36, 37, 42, 48] in responsive to the local tumor or endosomal environment. DOPE liposomes, in particular, can benefit from these lipopolymer constructs since DOPE is known to fuse with apposed lipid bilayers[49] and can be mixed with H_I-phase forming PEG-lipid conjugates to produce an L_α phase dispersion that resists membrane fusion. Once the PEG chains are detached by the triggering mechanism, however, the liposome becomes destabilized by the ensuing $L_\alpha \rightarrow H_{II}$ phase transition (Figure 1), thus promoting contents release and membrane fusion with adjacent membrane. This approach has been described using disulfide linked-[36, 37] and acid-sensitive orthoester-,[43] vinyl ether-[41, 42, 50] or hydrazone-[46]linked PEG-lipid conjugates. Studies with DOPE:mPEG-vinyl ether-lipid formulations showed that the contents release kinetics could be controlled by varying either the molar ratio of the mPEG-VE-lipid conjugate in the liposome membrane[42] or by altering the substitution pattern of the vinyl ether moiety.[50] These studies also showed, however, that only a limited range of kinetic timescales was accessible with these constructs, most of which were too slow for practical application in a drug delivery context. Development of PEG-lipids with controllable sensitivity is particularly important since there are many investigations showing that the observed pH

values of endosomes are time- and cell line-dependent. The measured pH within early (5 min) and late (8-10 min) endosomes of Chinese hamster ovary cells is 6.2 and 5.3, respectively.[51] The endosomal pH in mouse peritoneal macrophages decreased to 5.5 within 30-40 min,[52] whereas African green monkey kidney (CV-1) cells reach a similar pH within 3 h.[53] Confocal microscopy studies of KB cells showed that the endosomal pH varied between 4.7 and 5.8, with the pH in some endosomes dropping as low as 4.3.[54] Using a novel three-probe nanoparticle construction, Andresen and coworkers have shown that the endosomal pH of HepG2 cells varied widely between 3.8 and 6.5 over a 1.5 - 24 hr timeframe.[55, 56] These time and cell-line dependencies of endosomal pH indicates that the maximum efficacy of cytoplasmic contents release requires the optimization of liposomal acid sensitivity and fusogenicity inside target cells. This presents a significant design challenge since this must be achieved without altering the liposomal surface chemistry and composition that provides the necessary steric stabilization and plasma stability for effective targeting of the carrier *in vivo.*

In this work, we sought to develop mPEG-VE-DOG conjugates with a wide range of proton affinities to probe whether their respective hydrolysis rates were strongly correlated with their electronic, liposome cargo release, and liposome *in vivo* properties. Since the hydrolysis rates of simple vinyl ether model compounds are known to be strongly dependent on the substitution pattern and stereoelectronics of the linkage,[57-62] we designed a family of mPEG-VE-DOG conjugates bearing identical mPEG headgroups and lipid anchors to test whether the hydrolysis kinetics could be tuned as required for efficient liposomal cargo release at pH values found in early endosomal compartments. The design, synthesis, and hydrolysis rates of these conjugates, as well as their contents release rates, pharmacokinetics and biodistribution in DOPE liposome dispersions, are reported.

RESULTS & DISCUSSION

Design of Acid-Cleavable Vinyl Ether Linkages with Controlled Acid Sensitivity

Vinyl ether hydrolysis is known to proceed through a rate-determining proton transfer step to the β-carbon of the vinyl ether, followed by rapid hydration and rapid decomposition of a hemiacetal intermediate (Figure 2). Kresge and co-workers extensively searched for examples of vinyl ethers having a different rate-determining step, however, no exceptions to this mechanism were found.[58, 61-63] Vinyl acetals were considered as potentially exceptional cases to this pattern of rate-determining protonation step (r.d.s.) mechanisms, however, these reactions were found to proceed through acetal cleavage rather than vinyl ether hydrolysis,[64] indicating that the mechanism in Figure 2 is still valid. This pathway suggests that stabilization of the carbocation intermediate with electron releasing groups at α-position of the vinyl ether should increase the kinetics of the acid-catalyzed vinyl ether hydrolysis by lowering activation energy of carbocation formation. Conversely, destabilization of the intermediate by electron withdrawing groups should reduce the hydrolysis rate.

Several examples of previously reported second order acid-catalyzed hydrolysis rate constants of simple vinyl ether having different substituents at the α or β position are shown in Table 1, providing some insight into the potency of substituent effects on vinyl ether hydrolysis rates. Methyl substitution at the vinyl ether α-position increases the reactivity by a factor of 363 via stabilization of the carbocation intermediate, whereas an α-phenyl substituent increases the reactivity by only 70-fold. The relatively slow hydrolysis of the α-phenyl derivative can be attributed to stabilization of the vinyl ether starting material free energy via phenoxy conjugation, thus retarding the rate of carbocation intermediate formation by increasing the activation barrier toward protonation. α-Methoxy substitution confers dramatic increases in hydrolysis rate since the two methoxy groups greatly stabilize the carbocation intermediate after protonation, whereas very slow hydrolysis rates are

observed for methyl α-methoxyacrylate due to carbocation destabilization by the α-acyl group. Alkyl or phenyl substituents at the β-position of the vinyl ether destabilize the carbocation intermediate by electron withdrawing polar effects. The increased reactivity of the Z-methyl isomer relative to the E-isomer can be rationalized by the relative instability of the Z-isomer starting material due to steric strain (i.e. the activation barrier for hydrolysis is decreased, relative to the E-isomer, due to the higher energy Z form). Based on these observations, we sought the development of a structure-property relationship to enable the development of vinyl ether conjugates with *a priori* predictable hydrolysis rate constants.

Density Functional Theory as a Guide to PEG-VE-DOG Design

Ab initio methods have been used to calculate the proton affinities of a small series of methoxy-substituted methyl vinyl ethers and the results used to rationalize the relationship between the structure and reactivity of simple E-vs. Z-vinyl ethers.[60] To aid in design of the mPEG-VE-DOG conjugates with tunable acid-sensitivities needed for drug delivery applications, we employed density functional theory (DFT) calculations using the B3LYP hybrid functional[65, 66] to determine the proton affinities of vinyl ethers having various substituents at the α and/or β-carbon positions The structures of the vinyl ethers and their β-carbon protonated structures were optimized with the 6-31G** basis set and the single point energies optimized with the cc-pVTZ basis set. The vinyl ether proton affinities, determined as $PA = -\Delta rH_{298K}$ (SI, Table S1), were in reasonably good agreement with the reported intrinsic second order hydrolysis rate constants as a function of substituent type and position (Figure 3, $r^2 = 0.89$; SI, Table S2). In most cases, α-substituents exerted a greater influence on the proton affinity than the same substituent at the β-carbon.

Deviations from linearity in this structure-reactivity correlation may be attributed to experimental errors in the vinyl ether hydrolysis kinetics measurements as well as imperfect accounting for the steric and resonance effects by the proton affinity calculation. Nonetheless, this correlation provides a useful guide for the design of mPEG-VE-DOG conjugates having a range of acid sensitivities that are expected to vary across 11 orders of magnitude. Based on these computational inputs, we designed a family of mPEG-VE-DOGs (**ST912/ST915, ST902/ST905**, **ST502/ST505**, **ST302/305**, and **ST152/ST155**, Figure 4) bearing identical 1,2-dioleyl-*rac*-glyceryl lipid anchoring groups and mPEG2000 or mPEG5000 water-soluble polymer headgroups to enable a direct examination of the effects of vinyl ether reactivity on mPEG-VE-DOG hydrolysis, liposomal cargo release rate, and liposomal pharmacokinetics in mice.

Synthesis of mPEG-VE-DOG Lipids with Tunable Acid Sensitivity

While the structural motifs of the mPEG-VE-DOG lipid family are similar with respect to the membrane-associating 1,2-dioleyl-*rac*-glycerol lipid groups and the water-soluble mPEG headgroups, each vinyl ether type in this set of compounds required a separate synthesis pathway. **ST902** and **ST905** having a methyl ketene acetal linkage between the 1,2-dioleyl-*rac*-glycerol (DOG) and mPEG substituents were prepared by HI elimination[67] from methyl iodoacetal precursors (SI, Figure S1). **ST912** and **ST915**, having a ketene acetal linkage between DOG and mPEG, were prepared similarly (SI, Figure S2). **ST502** and **ST505**, containing an α-methylene substituted vinyl ether linkage between the DOG and mPEG moiety, were prepared by Tebbe olefination[68, 69] of a DOG-glycolate intermediate (SI, Figure S3). **ST302** and **ST305** were prepared as previously described by Shin *et al.*[50] **ST152** and **ST155**, having an α-amido substituted vinyl ether linkage between DOG and mPEG, were prepared via elimination from dimethylmalonate intermediates[70, 71] (SI, Figure S4).

Hydrolysis Kinetics of mPEG-VE-DOG Lipids

Hydrolysis kinetics of the mPEG-VE-DOG lipids was initially monitored by TLC using 8:1 CH_2Cl_2:MeOH (SI, Figure S5). These data showed that the mPEG-VE-lipid degradation rates followed the trend of **ST912/915** $\cong$ **ST902/905** > **ST502/505** > **ST302/305** > **ST152/155**, with the ST912/915 and ST902/905 compounds showing complete hydrolysis on the silica TLC plates used in the experiment.

Quantitative analysis of the hydrolysis rates was performed in acetate buffer (pH 3.0) via HPLC at a concentration of 10 mg/mL mPEG-VE-lipid. Samples of the reaction mixture were periodically removed, neutralized with 1M NaOH, the hydrolysis products extracted using the Bligh and Dyer method,[72] and the extract analyzed by HPLC. Rate constants were determined by plotting the ln[mPEG-VE-DOG] versus time. The intrinsic second order rate constants measured using this method (Table 2; SI, Figures S6-S10) were observed to be highly dependent on the substitution pattern of the mPEG-VE-DOG construct. **ST912** was found to have the fastest rate, intermediate rates were observed for **ST502/505** and **ST302/305**, while the slowest rates were measured for **ST152/155**. These findings are consistent with the qualitative TLC results, correlate well with the quantitative structure-activity relationship determined for vinyl ether model compounds (Figure 5), and suggest that α-substituents on the vinyl ether scaffold have a potent influence on their hydrolysis rates.

Contents Release Rates from DOPE:mPEG-VE-DOG Liposomes

Identical compositions and procedures were used to prepare DOPE:mPEG-VE-DOG liposome dispersions and analyze their contents release rates using the calcein fluorescence dequenching assay as described for **ST302** and **ST305**.[50] Liposomes containing encapsulated calcein were prepared and incubated at 37 °C in pH 3.5, 4.5, and 7.5 buffer solutions and their extent of contents release measured by fluorescence before and after addition of Triton X-100.

Dependence of Release Rate on Vinyl Ether Acid Sensitivity

The observed rates of calcein release from DOPE liposomes containing 10 mol% **ST912**, **ST502**, **ST302** and **ST152** are shown in Figures 6A-D, respectively. As expected, **ST912**-containing liposomes displayed the fastest calcein release in acidic media, with approximately 50% release occurring in less than 2 h at pH 3.5 and in 8 h at pH 4.5; however, extensive background leakage was also observed at pH 7.5 (~50% over 26 h). Rapid calcein release was also noted in **ST502**-containing liposome dispersions, with 50% release occurring over 4 h at pH 3.5 and 12 h at pH 4.5, while the background calcein release at pH 7.5 was minimal. **ST302**-containing liposomes displayed modest acid sensitivity, with exposure times of more than 48 h at pH 3.5 required to elicit 50% calcein release. These findings are consistent with the slow calcein efflux rates noted from DOPE:mPEG-VE-lipid dispersions that contained >3 mol% of mPEG-VE-lipid bearing an α-H,β-alkyl vinyl ether substitution pattern similar to **ST302**.[41, 42, 50] Very little contents release was observed from **ST152**-containing liposomes, even at pH 3.5 where less than 30% calcein release occurred after 48 h. Comparatively slower calcein release rates were observed relative to the measured hydrolysis rate constants due to the slow desorption of hydrolyzed mPEG from the DOPE-rich membrane in the absence of sink liposomes as previously reported.[24]

Subsequent investigations with the ketene acetal-based mPEG-lipid **ST912** sought to evaluate why the leakage rates were so fast at neutral pH. Reexamination of the fluorescence raw data showed that the ketene acetal liposomes typically contained 5 times less calcein than the other dispersion, even before they were exposed to acid. We attributed these results

to the high sensitivity of the ketene acetal derivatives to water. Unsubstituted ketene acetals are known to be hydrolyzed in non-acidic water-dioxane mixtures via a water-catalyzed reaction.[73] Hemiorthoester intermediates resulting from ketene acetal hydration has also been detected by ^{1}H NMR at −30 °C.[74, 75]

To examine the potential hydrolysis of ketene acetal-based mPEG-VE-DOG conjugates by neutral pH media, **ST912** and **ST902** containing small amounts of water, were dissolved in d_6-benzene from a freshly opened ampule and ^{1}H NMR spectra recorded over 36 h (SI, Figure S11). Hydrolysis of **ST912** was observed via the disappearance of the methylene peaks next to the ketene acetal moiety (3.9 ppm) with the simultaneous appearance of ester peaks arising from the hydrolyzed products (4.1-4.4 ppm). Slower hydrolysis of **ST902** was also observed, as expected, due to the anticipated lower reactivity of methyl substituted ketene acetal. This finding indicates that extensive **ST912** hydrolysis is occurring during the liposome preparation step and suggests that ketene acetal-linked mPEG-VE-DOG conjugates may not be useful for long-circulating liposomal drug delivery applications due to their high sensitivity to neutral conditions. Modulation of the ketene acetal acid sensitivity, e.g. by introduction of appropriate substituents on the β-carbon, will likely be required for the preparation of liposomes that are stable during the liposome preparation and blood circulation steps, but undergo fast contents release during the early endosomal acidification process within the target cells.

Dependence of Release Rate on mPEG-VE-DOG Molar Ratio

Extruded DOPE liposomes containing 5 mol% mPEG2000-VE-DOG and either 2, 5, or 8 mol% mPEG5000-VE-lipid were evaluated for their cargo release rates as a function of pH. Liposomes containing 5 mol% **ST152** produced ~48% leakage within 48 h at pH 3.5, with ~40% and 20% occurring within the same time period at pH 4.5 and 7.5, respectively (Figure 7A). When the mPEG molecular weight was increased to 5 kDa, the observed calcein leakage rates dropped to <20% for all pH's and **ST155** loadings evaluated (Figure 7B) and only reached ~40% for 2 mol% **ST305** at pH 3.5 (Figure S12E). We infer from these findings that a greater extent of mPEG5000-lipid hydrolysis is required to initiate the L_α-H_{II} phase transition and contents release from these liposomes. Most significantly; however, is the observation that calcein release rates are uniformly slow in the **ST152/5** series due to the slow rate of vinyl ether hydrolysis occurring in these dispersions, even pH 3.5, due to the electron deficiency of this vinyl ether construct relative to the other members of this series.

DOPE:**ST502** liposomes containing 5 mol% mPEG-VE-DOG lipid were more acid sensitive than the compositions containing higher loadings of **ST502**, with 50% calcein release observed at 1.5, 12.5 and >48 h at pH 3.5, 4.5 and 7.5, respectively (Figure 7C). A 2 mol% loading of **ST505** also produced rapid contents release under acidic conditions with minimal release at pH 7.5 (i.e., 50% release over 2 h at pH 3.5 and over 12 h at pH 4.5); however, increased loading of the PEG-lipid conjugates to 5 mol% and 8 mol% **ST505** decreased the observed calcein release to 50% over 6 h at pH 3.5 and >30 h at pH 4.5 (Figures 7D & S13B-D). The increased acid responsiveness of **ST502/5** liposomes relative to **ST152/5** and **ST302/5** is attributed to the higher proton affinity of the **ST502/5** vinyl ether motif containing an α-hydroxymethyl substituent.

Pharmacokinetics and Biodistribution of 90:10 DOPE:PEG-VE-lipid Liposomes in BALB/c Mice

The pharmacokinetic (PK) and biodistribution (BD) profile of 90:10 DOPE:mPEG-VE-DOG liposomes containing encapsulated [^{125}I]-TI and either **ST302** or **ST502**, was determined at 2 and 24 h following i.v. injection into the tail vein of mice at a phospholipid

dose of 0.5 μmol/mouse. Liposomes stabilized with 10 mol % **ST302** had longer circulation half-lives ($t_{1/2}$ of 7 h, 22% in blood at 24h) compared to those stabilized with 10 mol % **ST502** ($t_{1/2}$ of 3 h, 10% in blood at 24 h) (Figure 8).

At 2 h post-injection, over 90% of the ^{125}I for both liposomal formulations remained *in vivo*, indicating that the liposome contents were well retained at this time point. Both types of liposomes had high blood levels at 2 h post-injection, but evidence of initial clearance into liver and spleen was apparent (Figure 9A&B), with the DOPE:**ST502** liposomes having greater clearance into the MPS than DOPE:**ST302** liposomes (30% vs. 24% in liver and spleen at 2 h).

Both liposomal formulations were extensively cleared from the blood and were localized primarily with the liver, spleen, and carcass 24 h after injection (Figure 9A&B). The percentage of ^{125}I label retained in the body at 24 h was lower for the DOPE:**ST302** liposomes (76.6 ± 0.4 %) than for the DOPE:**ST502** liposomes (81.9 ± 0.1 %), suggesting that the former lost their contents more rapidly *in vivo*. Again the DOPE:**ST502** liposomes had higher clearance into the MPS organs of liver and spleen (66% vs 50% at 24 h).

Formulations of **ST302** and **ST502** containing 10 mol% mPEG-VE-lipid and 90 mol% DOPE were the only compositions studied since previous studies have shown that lower molar ratios of mPEG lipids in DOPE liposomes results in their rapid clearance from circulation.[27] Both liposome formulations tested had a biphasic pharmacokinetic profile, with the DOPE:**ST302** liposomes displaying a circulation half-life of approximately 7 h, which was significantly longer than the approximately 3 h circulation half-life of the **ST502** liposomes. We attribute the longer circulation time of 90:10 DOPE:**ST302** liposomes to the slower hydrolysis rate constant for the **ST302** derivative, such that less PEG-VE-lipid is lost from the liposome surface, thus making it more stable during circulation than the more rapidly hydrolyzed derivative, **ST502**.

We also found that both liposomal formulations tended to localize extensively within the liver and spleen 24 h post-injection. This finding is in accord with the biphasic pharmacokinetic profile of other PEG-modified liposomes.[76] The first phase is rapid and is believed to be a zero-order process involving rapid uptake of these liposomes by resident macrophages of the spleen and liver. Once the liposome-uptake mechanisms of these cells are saturated, the clearance becomes a first-order process, resulting in a gradual clearance of the liposomes from blood over a period of time.[77] Nonetheless, there appears to be some intrinsic affinity of such lipids specifically to sites in the liver and spleen. Whether these lipids are recognized by the resident immunocompetent cells found in these organs or are attracted to other cells found in these organs requires further investigation.

CONCLUSIONS

A rational approach to the design of PEGylated liposomes with tunable acid sensitivity has been demonstrated and the performance of their DOPE dispersions evaluated *in vitro* and *in vivo*. Initial DFT calculations for a collection of vinyl ethers with known intrinsic second order hydrolysis rate constants (k_H) was used to develop a quantitative structure-property relationship. This correlation was used to guide the design of ten different mPEG-VE-DOG lipids that were anticipated to have a wide range of hydrolysis rates. HPLC analysis of the acid-catalyzed hydrolysis kinetics for this family of compounds revealed that they provide a spectrum of kinetic response that varies by ~ 10^9. Specifically, we found that ketene acetal-based PEG-lipid conjugates (**ST912**, **ST915**, **ST902**, and **ST905**) are hydrolyzed very rapidly under acidic conditions ($k_H \sim 10^4$ M^{-1} sec^{-1}); however, they are also cleaved quickly under neutral conditions, limiting their utility in long-circulating carrier-based drug

delivery applications. Conversely, α-acyl-substituted vinyl ethers (**ST152** & **ST155**, k_H ~ $10^{-5} – 10^{-6}$ M^{-1} sec^{-1}) are very insensitive to mildly acidic conditions. Intermediate rates of acid-catalyzed hydrolysis were noted for the α-methylene-substituted (**ST502** & **ST505**, k_H ~10^2 M^{-1} sec^{-1}) and the β-alkyl-(Z)-vinyl ether-substituted (**ST302** & **ST305**, k_H ~10^{-2} $–10^{-3}$ M^{-1} sec^{-1}) mPEG-VE-DOG conjugates. Calcein release rates from DOPE liposomes containing these mPEG-VE-DOG lipid derivatives mirrored their hydrolysis kinetics – the most readily cleaved conjugates produced the fastest release rates, while the species possessing modest and slow hydrolysis rates form liposomes with either slow or very slow calcein efflux rates. DOPE liposome release rates also can be modulated by varying the DOPE:mPEG-VE-DOG lipid molar ratio. Taken together, our data show that liposomal contents release rates can be kinetically tuned on an *a priori* basis to a target solution pH by varying the electron density of the vinyl ether bond and that lipid composition provides an additional lever for control.

The *in vivo* performance of these PEG-VE-lipid derivatives suggests that they may be promising stabilizing agents for acid-sensitive DOPE liposomes when formulated at 90:10 DOPE:PEG-VE-DOG lipid ratios. **ST502**-stabilized DOPE liposomes show good differential sensitivity to pH 7.5 and 4.5 over 24 h, while **ST302**-stabilized DOPE liposomes have a long circulation half-life. Both these findings suggest that these liposomes should be investigated further for their ability to achieve cell kill in cytotoxicity experiments and for their ability to enhance survival of mice bearing tumor xenografts to assess their ability to improve the therapeutic effect of anticancer agents. Nonetheless, the variation in pharmacokinetic response noted for otherwise equivalent 90:10 DOPE:**ST502** and DOPE:**ST302** liposomes also may indicate a 'double-edged sword' for the *in vivo* use of long-circulating drug carrier systems bearing pH-sensitive (e.g., bioresponsive vinyl ether-,[50] ortho ester-,[44] acetal-,[78] and N-ethoxybenzylimidazole-[79]based constructs that all share a common reaction path upon rate-determining formation of the oxonium-stabilized carbocation intermediate in each respective reaction mechanism), disulfide,[48] or oxanorbornadiene[80] conjugates – where the strategies employed to accelerate the response kinetics of the system may simultaneously contribute to its reduced stability during circulation in blood.

EXPERIMENTAL METHODS

DFT Calculations

Density functional theory (DFT) calculations were performed as described in the Supplementary Information.

Materials

Column chromatography was performed using 230-400 mesh silica gel or 80-200 mesh alumina with analytical grade solvents. THF was distilled from sodium benzophenone ketyl. Benzene, CH_2Cl_2, CH_3CN, NEt_3, DMF, DMSO, and pyridine were distilled from CaH_2. All other chemical were used without further purification. Anhydrous $MgSO_4$ was typically used as a drying agent for acid insensitive compounds; anhydrous Na_2CO_3 was used for acid sensitive compounds. $CDCl_3$ was filtered through anhydrous Na_2CO_3 to remove traces of adventitious acid before preparation of NMR samples with acid-sensitive compounds. mPEG2000-NH_2 and mPEG5000-NH_2 were purchased from Shearwater Corporation (PDI ~ 1.01 for both). mPEG2000-OH and mPEG5000-OH were purchased from Aldrich (PDI ~ 1.1 for both). All solvents for HPLC analysis were of spectrophotometric grade and filtered through 0.2 μm filters before use. Citric acid and NaOH (ThermoFisher) were reagent grade and used as received from the supplier. 1,2-Dioleoyl-*sn*-glycero-3-phosphoethanolamine (DOPE) and the HPLC internal standard, 1-lauroyl-2-hydroxy-*sn*-glycero-3-

phosphatidylcholine, were purchased from Avanti Polar Lipids (Albaster, AL). Sephadex G-50 and Sepharose CL-4B were purchased from Pharmacia Biotech (Uppsala, Sweden). Sterile, pyrogen-free saline was purchased from Baxter (Toronto, ON, Canada) and was supplemented with 25 mM 4-(2-hydroxyethyl)-1-piperazineethanesulfonic acid, pH 7.4 (HEPES-buffered saline). $Na^{125}I$ was purchased from Mandel Scientific. The synthesis of tyraminylinulin (TI) and the preparation of [^{125}I]-TI (an aqueous space marker for liposomes) have been previously described.[81] Nuclepore polycarbonate membranes (0.08, 0.1 and 0.2 μm pore size) were purchased from Northern Lipids (Vancouver, BC). Calcein (93%, Fluka) was purchased from Sigma-Aldrich Canada (Oakville ON). All other chemicals were of analytical grade and purchased from Aldrich.

General Procedures for Synthesis

^{1}H and ^{13}C NMR spectra were recorded at 300 MHz and 75 MHz, respectively, in the Purdue University Center for Cancer Research's Interdepartmental NMR Facility. Chemical shifts are reported in ppm relative to the residual solvent peaks as the internal standard. MS (EI/CI/ESI) was performed by the Purdue University Center for Cancer Research's Campus-Wide Mass Spectrometry Center.

PEG-lipid Syntheses

The detailed synthesis procedures for **ST152**, **ST155**, **ST502**, **ST505**, **ST902**, **ST905**, **ST912**, **ST915** and all the associated reaction intermediates appear in Supplementary Information.

Lipid Hydrolysis Studies

Lipid hydrolysis rates were determined using 10 mg of mPEG-VE-DOG lipid, distributed as a dry thin lipid film in the bottom of a test tube, that was dissolved in 1 mL of buffer at 20 °C by vortex mixing. An internal lipid standard, 1-lauroyl-2-hydroxy-*sn*-glycero-3-phosphatidylcholine (LPC), was included in the thin lipid film before initiating dispersion and hydrolysis. At each time point, an aliquot was neutralized on an ice bath with 1M NaOH and extracted using the Bligh & Dyer[72] method before HPLC analysis of the organic phase. Briefly, the hydrolyzed lipid was extracted using $CHCl_3$:MeOH:H_2O, initially added at a ratio of 1:2:0.8, followed by the addition of $CHCl_3$ and H_2O to give a final ratio of 2:2:1.8. The organic phase was then removed, evaporated under a stream of N_2, and the extracted lipid dissolved in $CHCl_3$ at a concentration of 800 μg/mL immediately before HPLC analysis. The $CHCl_3$ use to redissolve the lipid extract was filtered through anhydrous K_2CO_3 immediately before use to remove any residual HCl in the solvent. Each mPEG-VE-DOG lipid sample was run in duplicate and the average concentration used for subsequent kinetic analysis.

HPLC Analysis of Lipid Hydrolysis Reactions

An Agilent 1200 HPLC, equipped with an Agilent Zorbax Eclipse C-8 column (4.6 × 150 mm, 5 μm particles), Agilent Zorbax Eclipse C-8 guard cartridges, an in-line vacuum degasser, column thermostat, diode array detector, and an ESA Corona chemical aerosol detector (CAD) was used for analysis of the lipid hydrolysis samples. mPEG2000-containing samples were eluted with a gradient of IPA:H_2O (45:55 → 95:5) over 25 min at a flow rate of 0.75 mL/min; an IPA:H_2O gradient (25:75 → 95:5) over 35 min at the same flow rate was used for mPEG5000-containing samples. The column temperature was maintained at 40 °C throughout the analysis using a column thermostat. The lipids in the extracts were detected by CAD and the data analyzed using the ChemStation software provided by the manufacturer. Chromatographic peaks assigned to the internal standard (mPEG2000 conditions: LPC, R_t = 7.7 min, DOG, R_t = 19.9 min; mPEG5000 conditions:

LPC, R_t = 13.5 min, DOG, R_t= 32.3 min) were verified by comparison with retention times determined for standard samples. The degree of lipid hydrolysis as a function of time was determined using peak areas normalized against the internal standard. Standard curves were used to evaluate the linearity and response ratio for the mPEG-VE-DOG lipid starting materials and the hydrolysis products; observed variations relative to internal standard were less than ± 2%. Pseudo-first order rate constants (s^{-1}) were determined by plotting the ln[mPEG-VE-lipid] versus time and the intrinsic second order rate constants $(M^{-1} s^{-1})$ were determined as the product of the pseudo-first order rate constants times the inverse of the proton concentration.

Liposome Preparation

A 50 mM DOPE lipid stock in benzene:methanol (95:5) solution was prepared from lyophilized DOPE powder. mPEG-VE-DOG lipid powder was weighed into a vial, dissolved in approximately 100 µL benzene:methanol (95:5), and the appropriate volume of this solution added to 20 µmol DOPE for the *in vitro* leakage study, or 30 µmol DOPE for the pharmacokinetic and biodistribution studies, to produce a 90:10 DOPE:PEG lipid molar ratio. Leakage studies using other DOPE:mPEG-VE-DOG lipid mixtures were prepared by withdrawing the relevant volumes of lipid component from the same stock solutions. The lipid mixture was frozen in LN_2 and lyophilized for 20-48 h. The lyophilized lipid powder was then hydrated in 1 mL of 20 mM calcein (in 25 mM Tris, 140 mM NaCl pH 8.5, osmolarity adjusted to 328 mOsmol) for the *in vitro* leakage study or 1 mL $[^{125}I]$-TI solution (in 25 mM Tris, 140 mM NaCl, pH 9.0) for the pharmacokinetic and biodistribution studies. After hydration of the lyophilized powder by five cycles of freeze-thaw-vortexing with 1 mL Tris·HCl buffer (25 mM Tris·HCl, 140 mM NaCl, pH 9.0), the solution was sequentially extruded through a series of polycarbonate filters with pore sizes ranging from 0.2 to 0.08 µm, using a 10 mL thermobarrel Lipex Extruder. The mean diameter of the liposomes (100-140 nm) was determined by dynamic light scattering using a Brookhaven BI-90 particle sizer. Immediately before determining leakage from the liposomes *in vitro*, the unentrapped dye was removed by Sephadex G-50 gel filtration chromatography in TrisQHCl buffer (25 mM TrisQHCl, 140 mM NaCl, pH 9.0). In the pharmacokinetic and biodistribution studies, free $[^{125}I]$-TI was removed by Sepharose CL-4B chromatography in pyrogen-free saline supplemented with 25 mM 4-(2-hydroxyethyl)-1-piperazineethanesulfonic acid, pH 7.4 (HEPES-buffered saline) and the most concentrated liposome fractions pooled for leakage analysis or injection (pharmacokinetics & biodistribution studies).

In vitro Liposome Leakage Experiments

All solutions were equilibrated at 37 °C for 10 min prior to mixing. A 100 µL aliquot of the liposome stock solution was added to 1.4 mL of 20 mM oxalate (pH 3.5), 20 mM citrate (pH 4.5), or 20 mM HEPES (pH 7.4) buffer. The liposome suspensions were maintained at 37 °C for the duration of the experiment. At various time points, 100 µL aliquot samples were removed and diluted with 2 mL HEPES-buffered saline (25 mM HEPES, 140 mM NaCl, pH 7.4). The fluorescence intensity (λ_{ex}= 490 nm, λ_{em}= 518 nm) was measured using an SLM-Aminco Model 8100 fluorimeter before and after the addition of 10 µL of 10% Triton X-100 solution. Percent calcein released was then calculated using the following formula:

$$\%\text{Calcein Released} = \frac{Ft_x - Ft_0}{Fmaxtx - Ft_0} \times 100\%,$$

where Ft_x is the calcein fluorescence at a given time point, Ft_0 is the calcein fluorescence at t = 0 h, and $Fmaxt_x$ is the calcein fluorescence after the addition of 10 μL 10% Triton X-100.[82] All calcein leakage results are expressed as the mean of duplicate measurements.

Pharmacokinetic and Biodistribution Studies

Female BALB/c mice (6-8 weeks) in the weight range of 21-25 g were obtained from the University of Alberta Health Sciences Laboratory Animal Services. Mice were injected via the tail vein with 200 μL HEPES-buffered saline containing 0.5 μmol (as determined by phosphate assay) of $[^{125}I]$-TI-loaded liposomes (1.1-2.4×10^5 cpm per mouse) with mean diameters (polydispersity) of 114 (0.223) nm for 90:10 DOPE:**ST302** liposomes and 111 (0.174) nm for 90:10 DOPE:**ST502** liposomes. At 2 h and 24 h post injection, groups of 3 mice were euthanized, and organs (liver, spleen, lung, heart, thyroid, and kidneys), blood samples, and the whole carcass were taken for gamma counting. The data was corrected for the blood volume of organs as described previously.[72] Blood and organ pharmacokinetics results are expressed as a percentage of total injected counts recovered at a given time point. Pharmacokinetic and biodistribution values are expressed as mean ± standard deviation. All animal studies were conducted in accordance with the Canadian Council on Animal Care Guidelines and Policies with approval from the Health Sciences Animal Policy and Welfare Committee for the University of Alberta.

Supplementary Material

Refer to Web version on PubMed Central for supplementary material.

Acknowledgments

REFERENCES

1. Bangham AD, Standish MM, Watkins JC. Diffusion of univalent ions across the lamellae of swollen phospholipids. J. Mol. Biol. 1965; 13:238–252. [PubMed: 5859039]

2. Duncan R, Gaspar R. Nanomedicine(s) under the microscope. Mol. Pharm. 2011; 8:2101–2141. [PubMed: 21974749]

3. Mayer LD, Bally MB, Hope MJ, Cullis PR. Uptake of antineoplastic agents into large unilamellar vesicles in response to a membrane potential. Biochim. Biophys. Acta. 1985; 816:294–302. [PubMed: 3839135]

4. Mayer LD, Cullis PR, Bally MB. Uptake of adriamycin into large unilamellar vesicles in response to a pH gradient. Biochim. Biophys. Acta. 1986; 857:123–126. [PubMed: 3964703]

5. Lasic DD, Frederik PM, Stuart MC, Barenholz Y, McIntosh TJ. Gelation of liposome interior: a novel method for drug encapsulation. FEBS Lett. 1992; 312:255–258. [PubMed: 1426260]

6. Haran G, Cohen R, Bar LK, Barenholz Y. Transmembrane ammonium sulfate gradients in liposomes produce efficient and stable entrapment of amphipathic weak bases. Biochim. Biophys. Acta. 1993; 1151:201–215. [PubMed: 8373796]

7. Drummond DC, et al. Development of a highly stable and targetable nanoliposomal formulation of topotecan. J. Controlled Release. 2010; 141:13–21.

8. Peer D, Margalit R. Loading mitomycin C inside long circulating hyaluronan targeted nano-liposomes increases its antitumor activity in three mice tumor models. Int. J. Cancer. 2004; 108:78–789. [PubMed: 14618619]

9. Chen H, et al. Lipid encapsulation of arsenic trioxide attenuates cytotoxicity and allows for controlled anticancer drug release. J. Am. Chem. Soc. 2006; 128:13348–13349. [PubMed: 17031934]

10. Chen H, Ahn R, Van den Bossche J, Thompson DH, O'Halloran TV. Folate-mediated intracellular drug delivery increases the anticancer efficacy of nanoparticulate formulation of arsenic trioxide. Mol. Cancer Ther. 2009; 8:1955–1963. [PubMed: 19567824]

11. Petersen AL, et al. ^{64}Cu loaded liposomes as positron emission tomography imaging agents. Biomaterials. 2011; 32:2334–2341. [PubMed: 21216003]

12. Hope MJ, Bally MB, Webb G, Cullis PR. Production of large unilamellar vesicles by a rapid extrusion procedure. Characterization of size distribution, trapped volume and ability to maintain a membrane potential. Biochim. Biophys. Acta. 1985; 812:55–65. [PubMed: 23008845]

13. Matsumura Y, Maeda H. A new concept for macromolecular therapeutics in cancer chemotherapy: mechanism of tumoritropic accumulation of proteins and the antitumor agent SMANCS. Cancer Res. 1986; 46:6387–6392. [PubMed: 2946403]

14. Jain RK. Delivery of molecular and cellular medicine to solid tumors. Adv. Drug Del. Rev. 2001; 46:149–168.

15. Maeda H. Tumor-selective delivery of macromolecular drugs via the EPR effect: background and future prospects. Bioconjugate Chem. 2010; 21:797–802.

16. Leserman LD, Barbet J, Kourilsky F, Weinstein JN. Targeting to cells of fluorescent liposomes covalently coupled with monoclonal antibody or protein A. Nature. 1980; 288:602–604. [PubMed: 7442804]

17. Heath TD, Fraley RT, Papahadjopoulos D. Antibody targeting of liposomes: cell specificity obtained by conjugation of F(ab')$_2$ to vesicle surfaces. Science. 1980; 210:539–541. [PubMed: 7423203]

18. Howard WA, et al. Sonolysis promotes indirect Co-C bond cleavage of alkylcob(III)alamin bioconjugates. Bioconjugate Chem. 1997; 8:498–502.

19. Rui Y, Wang S;S, Low PS, Thompson DH. Diplasmenylcholine-folate liposomes: An efficient vehicle for intracellular drug delivery. J. Am. Chem. Soc. 1998; 120:11213–11218.

20. Hussain S, Pluckthun A, Allen TM, Zangemeister-Wittke U. Antitumor activity of an epithelial cell adhesion molecule-targeted nanovesicular drug delivery system. Mol. Cancer Ther. 2007; 6:3019–3027. [PubMed: 18025286]

21. Sega EI, Low PS. Tumor detection using folate receptor-targeted imaging agents. Cancer Metast. Rev. 2008; 27:655–664.

22. Qualls MM, Thompson DH. Chloroaluminum phthalocyanine tetrasulfonate delivered via acid-labile diplasmenylcholine-folate liposomes: Intracellular localization and synergistic phototoxicity. Int. J. Cancer. 2001; 93:384–392. [PubMed: 11433404]

23. Guo X, MacKay JA, Szoka FC. Mechanism of pH-triggered collapse of phosphatidylethanolamine liposomes stabilized by an ortho ester polyethyleneglycol lipid. Biophys. J. 2003; 84:1784–1795. [PubMed: 12609880]

24. Boomer JA, et al. Cytoplasmic delivery of liposomal contents mediated by an acid-labile cholesterol-vinyl ether-PEG conjugate. Bioconjugate Chem. 2009; 20:47–59.

25. Qin S, et al. An imaging-driven model for liposomal stability and circulation. Mol. Pharm. 2009; 7:12–21. [PubMed: 19621944]

26. Park JW, et al. Anti-HER2 immunoliposomes: enhanced efficacy attributable to targeted delivery. Clin. Cancer Res. 2002; 8:1172–1181. [PubMed: 11948130]

27. Charrois GJR, Allen TM. Rate of biodistribution of STEALTH liposomes to tumor and skin: influence of liposome diameter and implications for toxicity and therapeutic activity. Biochim. Biophys. Acta. 2003; 1609:102–108. [PubMed: 12507764]

28. Webb MS, et al. A cationic liposomal vincristine formulation with improved vincristine retention, extended circulation lifetime and increased anti-tumor activity. Lett. Drug Des. Disc. 2007; 4:426–433.

29. Silvius JR, Zuckermann MJ. Interbilayer transfer of phospholipid-anchored macromolecules via monomer diffusion. Biochemistry. 1993; 32:3153–3161. [PubMed: 7681327]

30. Holland JW, Cullis PR, Madden TD. Poly(ethylene glycol)-lipid conjugates promote bilayer formation in mixtures of non-bilayer-forming lipids. Biochemistry. 1996; 35:2610–2617. [PubMed: 8611564]

31. Mori A, et al. Stabilization and regulated fusion of liposomes containing a cationic lipid using amphipathic polyethyleneglycol derivatives. J. Liposome Res. 1998; 8:195–211.

32. Adlakha-Hutcheon G, Bally MB, Shew CR, Madden TD. Controlled destabilization of a liposomal drug delivery system enhances mitoxantrone antitumor activity. Nature Biotechnol. 1999; 17:775–779. [PubMed: 10429242]

33. Li WM, Zue L, Mayer LD, Bally MB. Intermembrane transfer of a polyethylene glycol-modified phosphatidylethanolamine as a means to reveal surface-associated binding ligands on liposomes. Biochim. Biophys. Acta. 2001; 1513:193–206. [PubMed: 11470091]

34. Hu Q, Shew CR, Bally MB, Madden TD. Programmable fusogenic vesicles for intracellular delivery of antisense oligodeoxynucleotides: enhanced cellular uptake and biological effects. Biochim. Biophys. Acta. 2001; 1514:1–13. [PubMed: 11513800]

35. Auguste DT, Prud'homme RK, Ahl PL, Meers P, Kohn J. Association of hydrophobically-modified poly(ethylene glycol) with fusogenic liposomes. Biochim. Biophys. Acta. 2003; 1616:184–195. [PubMed: 14561476]

36. Kirpotin D, Hong KL, Mullah N, Papahadjopoulos D, Zalipsky S. Liposomes with detachable polymer coating: destabilization and fusion of dioleoylphosphatidylethanolamine vesicles triggered by cleavage of surface-grafted poly(ethylene glycol). FEBS Lett. 1996; 388:115–118. [PubMed: 8690067]

37. Zalipsky S, et al. New detachable poly(ethylene glycol) conjugates: cysteine-cleavable lipopolymers regenerating natural phospholipid, diacylphosphatidylethanolamine. Bioconjugate Chem. 1999; 10:703–707.

38. Ishida T, Kirchmeier MJ, Moase EH, Zalipsky S, Allen TM. Targeted delivery and release of liposomal doxorubicin enhances cytotoxicity against human B lymphoma cells. Biochim. Biophys. Acta. 2001; 1515:144–158. [PubMed: 11718670]

39. Andresen TL, Thompson DH, Kaasgaard T. Enzyme-triggered nanomedicine: drug release strategies in cancer therapy. Mol. Memb. Biol. 2010; 27:353–363.

40. Gerasimov OV, Boomer JA, Qualls MM, Thompson DH. Cytosolic drug delivery using pH- and light-sensitive liposomes. Adv. Drug Del. Rev. 1999; 38:317–338.

41. Bergstrand N, Arfvidsson MC, Kim J-M, Thompson DH, Edwards K. Interactions between pH-sensitive liposomes and model membranes. Biophys. Chem. 2003; 104:361–379. [PubMed: 12834854]

42. Boomer JA, et al. Acid-triggered release from sterically-stabilized fusogenic vesicles via a hydrolytic dePEGylation strategy. Langmuir. 2003; 19:6408–6415.

43. Guo X, Szoka FC. Steric stabilization of fusogenic liposomes by a low-pH sensitive PEG-diortho ester-lipid conjugate. Bioconjugate Chem. 2001; 12:291–300.

44. Li WJ, Huang ZH, MacKay JA, Grube S, Szoka FC. Low-pH-sensitive poly(ethylene glycol) (PEG)-stabilized plasmid nanolipoparticles: effects of PEG chain length, lipid composition and assembly conditions on gene delivery. J. Gene Med. 2005; 7:67–79. [PubMed: 15515149]

45. MacKay JA, et al. HIV TAT peptide modifies the distribution of DNA nanolipoparticles following convection-enhanced delivery. Mol. Ther. 2008; 16:893–900. [PubMed: 18388927]

46. Kale AA, Torchilin VP. Design, synthesis, and characterization of pH-sensitive PEG-PE conjugates for stimuli-sensitive pharmaceutical nanocarriers: the effect of substitutes at the hydrazone linkage on the pH stability of PEG-PE conjugates. Bioconjugate Chem. 2007; 18:363–370.

47. Biswas S, Dodwadkar NS, Sawant RR, Torchilin VP. Development of the novel PEG-PE-based polymer for reversible attachment of specific ligands to liposomes: synthesis and in vitro characterization. Bioconjugate Chem. 2011; 22:2005–2013.

48. Zhang JX, Zalipsky S, Mullah N, Pechar M, Allen TM. Pharmaco attributes of dioleoylphosphatidylethanolamine/cholesterolhemisuccinate liposomes containing different types of cleavable lipopolymers. Pharm. Res. 2004; 49:185–198.

49. Ellens H, Bentz J, Szoka FC. Fusion of phosphatidylethanolamine-containing liposomes and mechanism of the La-HII phase transition. Biochemistry. 1986; 25:4141–4147. [PubMed: 3741846]

50. Shin J, Shum P, Thompson DH. Acid-triggered release via dePEGylation of DOPE liposomes containing acid-labile vinyl ether PEG-lipids. J. Controlled Release. 2003; 91:187–200.

51. Schmid S, Fuchs R, Kielian M, Helenius A, Mellman I. Acidification of endosome subpopulations in wild-type Chinese hamster ovary cells and temperature-sensitive acidification-defective mutants. J. Cell Biol. 1989; 108:1291–1300. [PubMed: 2925786]

52. Daleke DL, Hong KL, Papahadjopoulos D. Endocytosis of liposomes by macrophages - binding, acidification and leakage of liposomes monitored by a new fluorescence assay. Biochim. Biophys. Acta. 1990; 1024:352–366. [PubMed: 2162207]

53. Straubinger RM, Papahadjopoulos D, Hong K. Endocytosis and intracellular fate of liposomes using pyranine as a probe. Biochemistry. 1990; 29:4929–4939. [PubMed: 2163672]

54. Lee RJ, Wang S, Low PS. Measurement of endosome pH following folate receptor-mediated endocytosis. Biochim. Biophys. Acta. 1996; 1312:237–242. [PubMed: 8703993]

55. Sun HH, Andresen TL, Benjaminsen RV, Almdal K. Polymeric nanosensors for measuring the full dynamic pH range of endosomes and lysosomes in mammalian cells. J. Biomed. Nanotech. 2009; 5:676–682.

56. Benjaminsen RV, et al. Evaluating nanoparticle sensor design for intracellular pH measurements. ACS Nano. 2011; 5:5864–5873. [PubMed: 21707035]

57. Cooper JD, Vitullo VP, Whalen DL. Evidence for a change in rate determining step in acid-catalyzed hydrolysis of a vinyl ether. J. Am. Chem. Soc. 1971; 93:6294–6296.

58. Keeffe, JR.; Kresge, AJ. The Chemistry of Enols. Rappoport, Z., editor. Vol. 437. John Wiley & Sons; New York, NY: 1990.

59. Kresge AJ, Tobin JB. Vinyl ether hydrolysis. 25 Effect of alpha-trimethylsilyl and beta-trimethylsilyl substitution. J. Phys. Org. Chem. 1991; 4:587–591.

60. Leibovitch M, Kresge AJ, Peterson MR, Csizmadia IG. Ab initio investigation of the structure and reactivity of vinyl ethers. THEOCHEM. 1991; 76:349–385.

61. Kresge AJ, Leibovitch M. Kinetics and mechanism of the acid-catalyzed hydrolysis of 1,1-dimethoxyethene (ketene dimethyl acetal) and trimethoxyethene in aqueous solution. J. Am. Chem. Soc. 1992; 114:3099–3102.

62. Kresge AJ, Leibovitch M, Sikorski JA. Acid-catalyzed hydrolysis of 5-enolpyruvylshikimate 3-phosphate (EPSP) and some simple models of its vinyl ether functional group. J. Am. Chem. Soc. 1992; 114:2618–2622.

63. Kresge AJ, Sagatys DS, Chen HL. Vinyl ether hydrolysis. 9 Isotope effects on proton transfer from hydronium ion. J. Am. Chem. Soc. 1977; 99:7228–7233.

64. Chiang Y, Chwang WK, Kresge AJ, Yin Y. Acid-catalyzed hydrolysis of vinyl acetals. Reaction through the acetal rather than the vinyl ether functional group. J. Am. Chem. Soc. 1989; 111:7185–7190.

65. Becke AD. Density-functional thermochemistry. 3 The role of exact exchange. J. Chem. Phys. 1993; 98:5648–5652.

66. Lee CT, Yang WT, Parr RG. Development of the Colle-Salvetti correlation energy formula into a functional of the electron density. Phys. Rev. B. 1988; 37:785–789.

67. Middleton DS, Simpkins NS. A mild method for the preparation of functionalized, unsymmetrical ketene acetals. Syn. Comm. 1989; 19:21–29.

68. Okazoe T, Takai K, Oshima K, Utimoto K. Alkylidenation of ester carbonyl groups by means of a reagent derived from $RCHBr_2$, Zn, $TiCl_4$ and TMEDA - stereoselective preparation of (Z)-alkenyl ethers. J. Org. Chem. 1987; 52:4410–4412.

69. Takai K, Kakiuchi T, Kataoka Y, Utimoto K. Novel catalytic effect of lead on the reduction of a zinc carbenoid with zinc metal leading to a geminal dizinc compound - acceleration of the Wittig-type olefination with $RCHX_2$-$TiCl_4$-Zn systems by addition of lead. J. Org. Chem. 1994; 59:2668–2670.

70. Baum JS, Shook DA, Davies HML, Smith HD. Diazotransfer reactions with p-acetamidobenzenesulfonyl azide. Syn. Comm. 1987; 17:1709–1716.

71. Bartlett PA, Maitra U, Chouinard PM. Synthesis of iso-EPSP and evaluation of its interaction with chorismate synthase. J. Am. Chem. Soc. 1986; 108:8068–8071.

72. Bligh EG, Dyer WJ. A rapid method of total lipid extraction and purification. Can. J. Biochem. Physiol. 1959; 37:911–917. [PubMed: 13671378]

73. Kankaanpera A, Aaltonen R. General acid-catalyzed hydrolysis of unsubstituted ketene acetals. Acta Chem. Scand. 1972; 26:1698–1706.

74. Capon B, Ghosh AK. Tetrahedral intermediates. 2 The detection of hemiorthoesters in the hydration of ketene acetals and the mechanism of their breakdown. J. Am. Chem. Soc. 1981; 103:1765–1768.

75. Capon B, Dosunmu MI. Tetrahedral intermediates. 4 The effect of chloro substituents on the kinetics of the breakdown of hemiorthoesters. Tetrahedron. 1984; 40:3625–3633.

76. Koning GA, et al. Pharmacokinetics of differently designed immunoliposome formulations in rats with or without hepatic colon cancer metastases. Pharm. Res. 2001; 18:1291–1298. [PubMed: 11683242]

77. Allen TM. Liposomal drug formulations - rationale for development and what we can expect in the future. Drugs. 1998; 56:747–756. [PubMed: 9829150]

78. Gillies ER, Goodwin AP, Frechet JMJ. Acetals as pH-sensitive linkages for drug delivery. Bioconjugate Chem. 2004; 15:1254–1283.

79. Kong SD, Luong A, Manorek G, Howell SB, Yang J. Acidic hydrolysis of N-ethoxybenzylimidazoles (NEBIs): potential applications as pH-sensitive linkers for drug delivery. Bioconjugate Chem. 2007; 18:293–296.

80. Kislukhin AA, Higginson CJ, Hong VP, Finn MG. Degradable conjugates from oxanorbornadiene reagents. J. Am. Chem. Soc. 2012; 134:6491–6497. [PubMed: 22455380]

81. Sommerman EF, Pritchard PH, Cullis PR. ^{125}I-labeled inulin: a convenient marker for deposition of liposomal contents in vivo. Biochem. Biophys. Res. Comm. 1984; 122:319–324. [PubMed: 6743334]

82. Allen TM, Hong K, Papahadjopoulos D. Membrane contact, fusion and hexagonal (HII) transitions in phosphatidylethanolamine liposomes. Biochemistry. 1990; 29:2976–2985. [PubMed: 2337577]
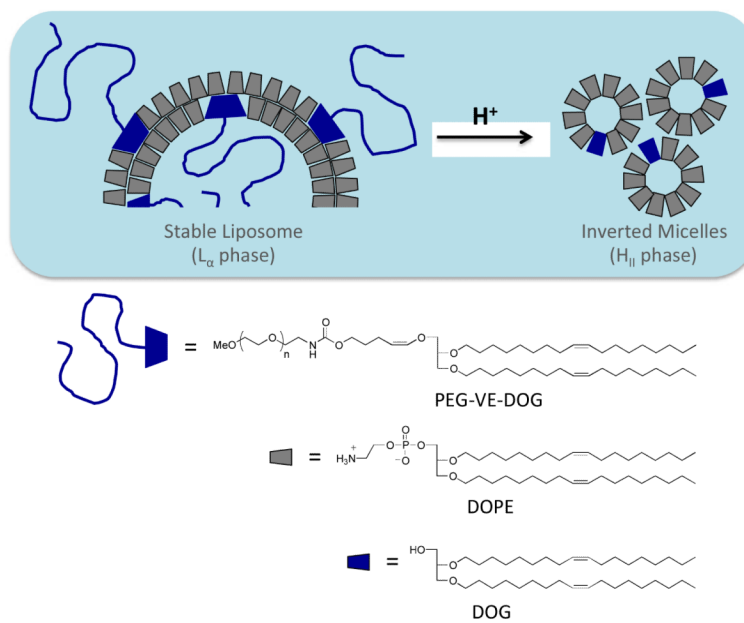
Figure 1.
Conceptual diagram of L_α-H_{II} phase transition induced by acid-catalyzed dePEGylation of DOPE:PEG-VE-lipid liposomes via conversion of the H_I phase PEG-VE-lipid into the H_{II} phase DOG hydrolysis product.
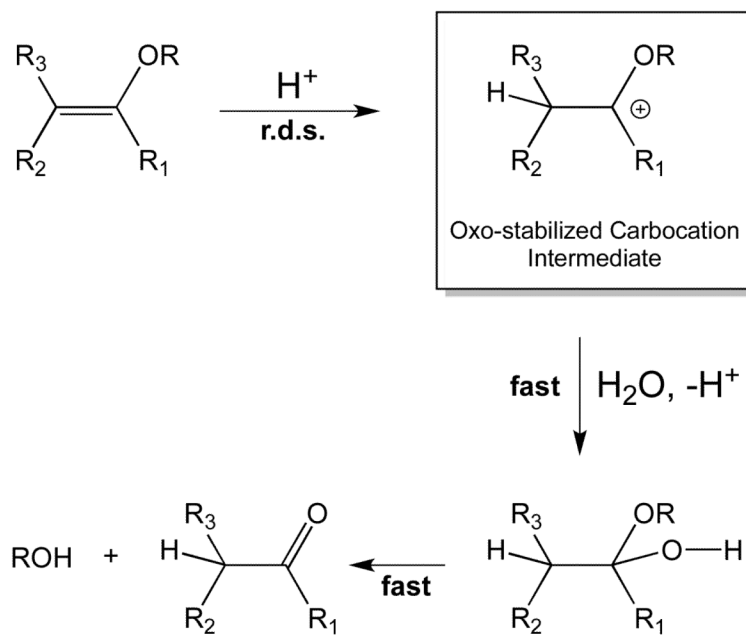
Figure 2.
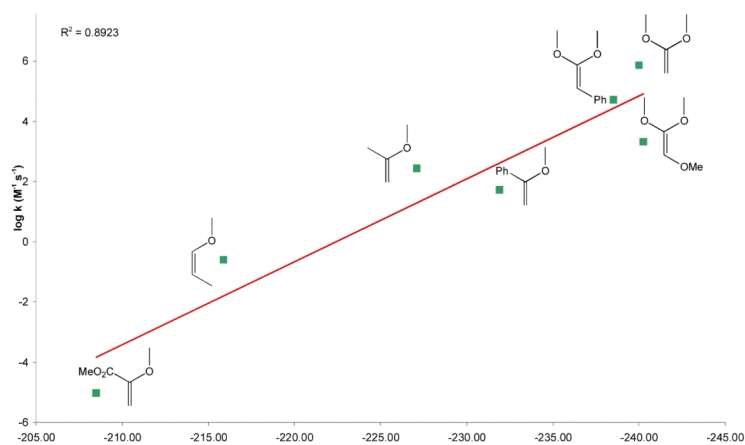Mechanism of acid-catalyzed vinyl ether hydrolysis.

Figure 3.
Structure-activity relationship for known vinyl ethers. Intrinsic second order rate constants $(M^{-1} \cdot s^{-1})$ versus DFT proton affinities (kcal/mol) calculated for the vinyl ethers shown.

ST912 (n ~ 45); **ST915** (n ~ 114)

ST902 (n ~ 45); **ST905** (n ~ 114)

ST502 (n ~ 45); **ST505** (n ~ 114)

ST302 (n ~ 45); **ST305** (n ~ 114)

ST152 (n ~ 45); **ST155** (n ~ 114)
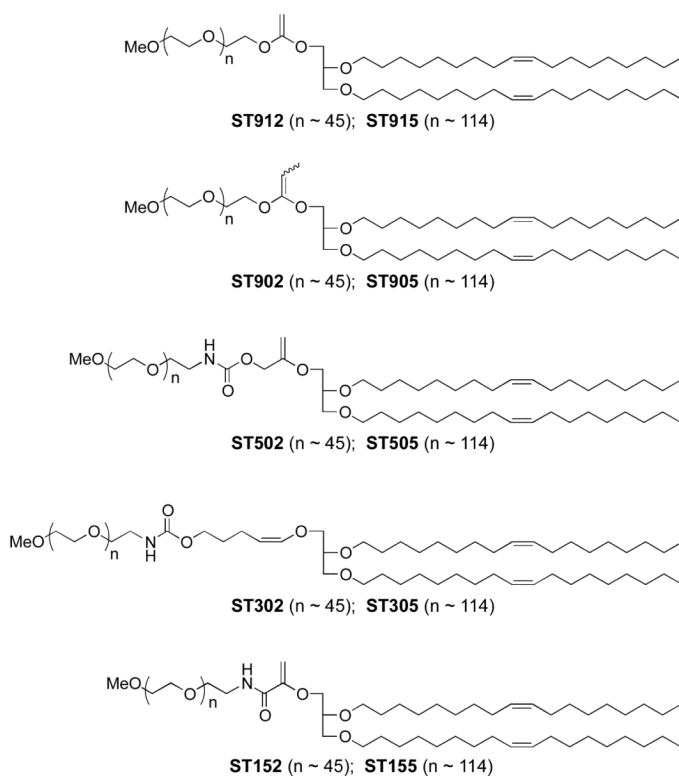
Figure 4.
Family of 3-(methoxypolyethylene glycol)-vinyl ether-1,2-dioleylglycerol conjugates with variable electron demand synthesized for evaluation in acid-sensitive fusogenic liposome formulations.
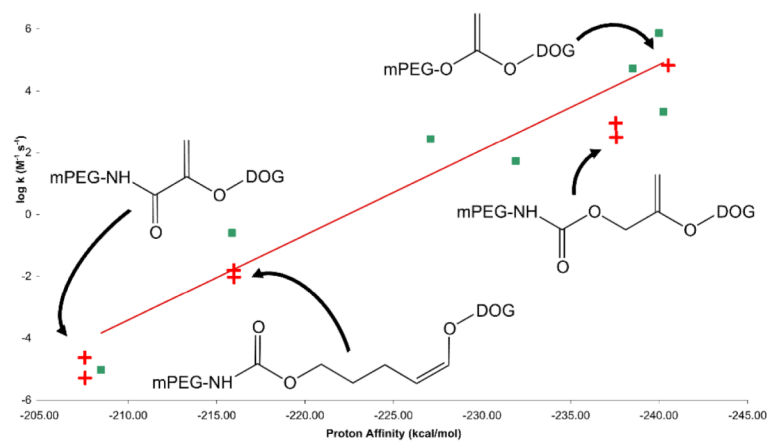
Figure 5.
Correlation of mPEG-VE-Lipid Hydrolysis Rates and Proton Affinities with the Vinyl Ether SAR from Figure 4.
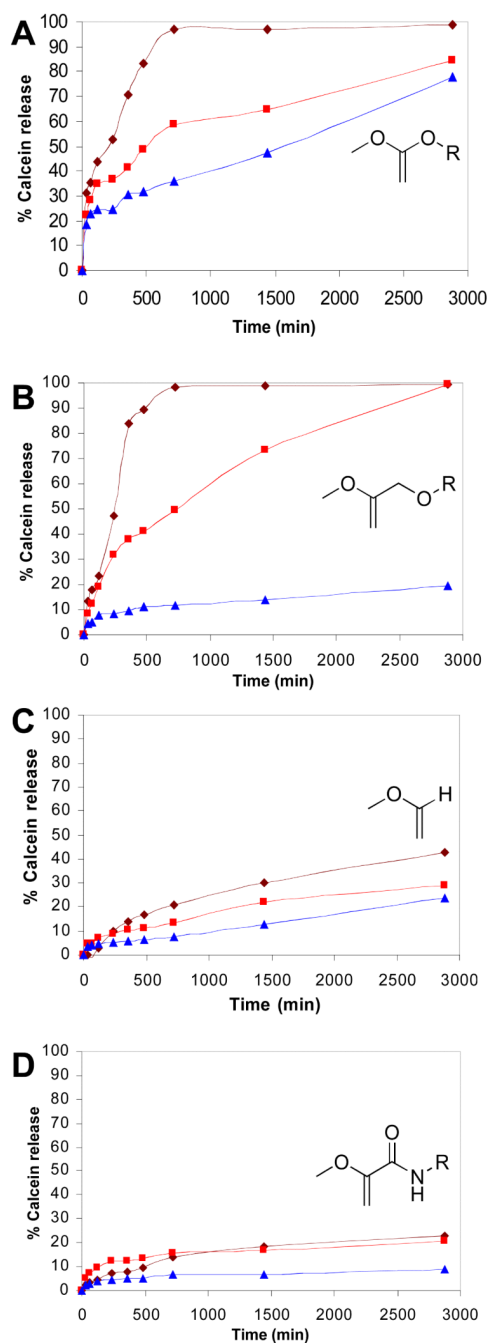
Figure 6.
Calcein release rates at 37 °C for extruded 90:10 DOPE:PEG-VE-DOG liposome dispersions as a function of solution pH. **A**: DOPE:**ST912**. **B**: DOPE:**ST502**. **C**: DOPE:**ST302** (reproduced from ref. 50). **D**: DOPE:**ST152**. Lines and points on all graphs: dark red = pH 3.5; light red = pH 4.5; blue = pH 7.5.
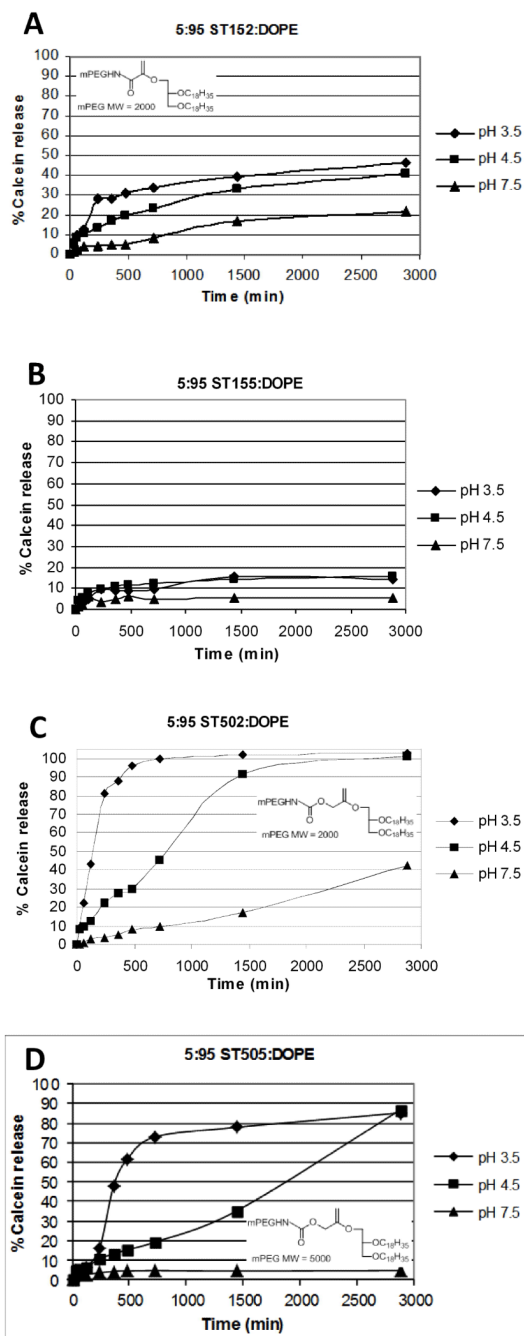
Figure 7.
Calcein release rates at 37 °C for extruded 5:95 DOPE:PEG-VE-DOG liposome dispersions as a function of solution pH. **A**: DOPE:**ST152**. **B**: DOPE:**ST155**. **C**: DOPE:**ST502**. **D**: DOPE:**ST505**.
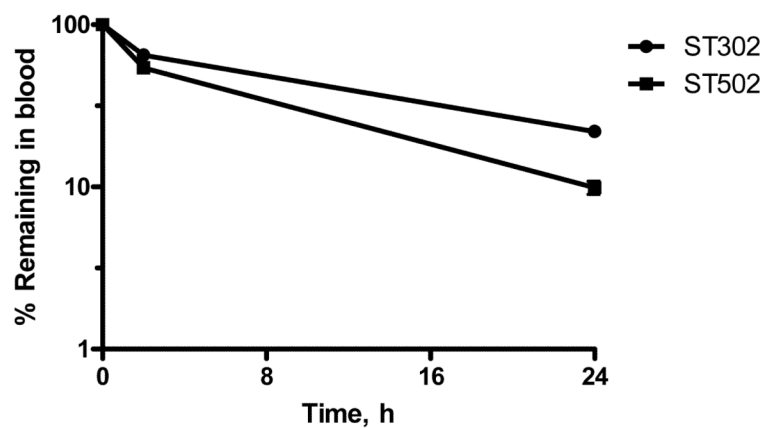
Figure 8.
Pharmacokinetics of 90:10 DOPE:**ST302** (■) or 90:10 DOPE:**ST502** (◆) liposomes in BALB/c mice. Female BALB/c mice were injected i.v. via the tail vein with a single dose of 0.5 Zmol phospholipids as [^{125}I]-TI encapsulated DOPE liposomes stabilized with 10 mol % ST302, in 0.2 mL volume. At 2 h and 24 h after injection, blood samples were collected and counted for ^{125}I. Recovery of counts in the blood was calculated assuming a total blood volume of 7.5% of mouse weight, and results are expressed as a percent of the total counts remaining in the mouse at that time point. Results are means of triplicate analyses ± SD.
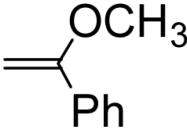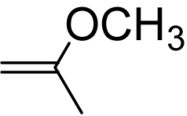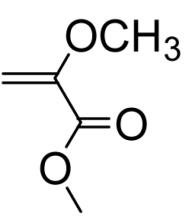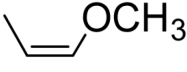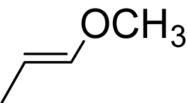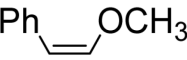
A

B
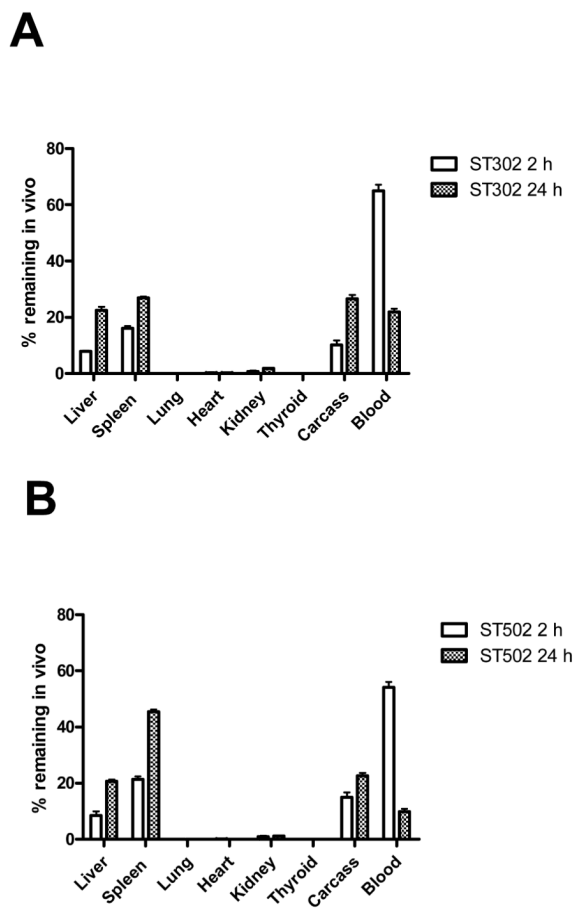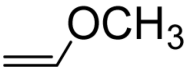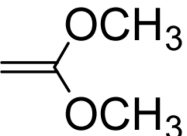
Figure 9.
Biodistribution of liposomes, 2 h and 24 h post-injection. **(A)** 90:10 DOPE:**ST302**
liposomes. **(B)** 90:10 DOPE:**ST502** liposomes. Female BALB/c mice were injected *i.v.* via
the tail vein with a single dose of 0.2 ml of [^{125}I]-TI encapsulated DOPE liposomes
stabilized with 10 mol % **ST302** or **ST502**. At 2 h and 24 h after injection, mice were
euthanized, and blood, various organs, and the carcass were collected and counted for ^{125}I.
Standard blood correction factors were applied to correct for blood in organs and carcass.
Results are expressed as a percentage of the total counts remaining in the mouse, and are the
means of triplicate analyses ± SD.

Table 1

Intrinsic Second Order Hydrolysis Rate Constants for a Related Series of Simple Vinyl Ethers.

Vinyl Ethers	k_H (M^{-1}s^{-1})	Relative Rates
[structure: CH$_2$=CH–OCH$_3$]	0.760[a]	1
[structure: CH$_2$=C(Ph)–OCH$_3$]	53.3[b]	70.1
[structure: CH$_2$=C(CH$_3$)–OCH$_3$]	276[c]	363
[structure: CH$_2$=C(OCH$_3$)–OCH$_3$]	720000[d]	947000
[structure: CH$_2$=C(OCH$_3$)–CO–O–CH$_3$]	0.0000094[e]	0.0000124
[structure: cis CH$_3$CH=CH–OCH$_3$]	0.255[a]	0.336
[structure: trans CH$_3$CH=CH–OCH$_3$]	0.072[a]	0.0947
[structure: Ph–CH=CH–OCH$_3$]	0. 00267[f]	0.00351

[a] Kresge *et al.* (1977);

[b] Chiang *et al.* (1978);

[c] Keefe & Kresge (1990);

[d] Kresge & Leibovitch (1992);

[e] Kresge *et al.* (1992);

[f] Chiang et al. (1978).

Table 2

Calculated Proton Affinities and Measured Intrinsic Second Order Rate Constants for mPEG-VE-DOG Lipids with Varying Electronic Properties

mPEG-VE-Lipid	Proton Affinity (kcal/mol)	Second Order Rate Constant (M^{-1} sec^{-1})
ST912	−240.26	5.2×10^4
ST502	−237.32	730
ST505	"	240
ST302	−215.88	1.4×10^{-2}
ST305	"	8.3×10^{-3}
ST152	−207.5[1]	5×10^{-6}
ST155	"	2.5×10^{-5}